European Journal of Applied Sciences – Vol. 13, No. 02
Publication Date: April 25, 2025
DOI:10.14738/aivp.1302.18429.
Mawuli, S. E., Anthony, S., & Akintunde, D. O. (2025). Characterization of Periwinkle Shell Powder as a Possible Replacement for Asbestos in the Production of Automotive Disc Brake Linings. European Journal of Applied Sciences, Vol - 13(02). 106-118.

Characterization of Periwinkle Shell Powder as a Possible Replacement for Asbestos in the Production of Automotive Disc Brake Linings

Seckley Emmanuel Mawuli
Department of Mechanical Engineering,
University of Mines and Technology, Tarkwa, Ghana

Simons Anthony
Department of Mechanical Engineering,
University of Mines and Technology, Tarkwa, Ghana

Dahunsi Olurotimi Akintunde
Department of Mechanical Engineering,
The Federal University of Technology, Akure, Nigeria

ABSTRACT

This study investigates the potential of Periwinkle Shell (PS) powder as a substitute for asbestos in friction lining materials, given the carcinogenic nature of asbestos. Periwinkle, a small univalve gastropod mollusk, specifically *Tympanotonos fuscatus* (commonly called the West African Mud Creeper), is explored for its suitability in industries like construction and brake pad manufacturing. However, there is limited research on the properties of periwinkle shell. To address this gap, the study characterizes the PS powder using a range of tests, including mechanical testing, X-ray Diffraction (XRD), X-ray Fluorescence (XRF), Differential Scanning Calorimetry-Thermogravimetric Analysis (DSC-TGA), and Scanning Electron Microscopy-Energy Dispersive Spectroscopy (SEM-EDS). The findings show that the density of PS powder (1.316 g/cm^3 for untapped bulk density and 1.718 g/cm^3 for dry bulk density) is lower than that of asbestos, which has a density of 2.22 g/cm^3. Additionally, the chemical and mineralogical compositions of PS powder are similar to asbestos, both containing silica, calcite, anhydrite, and quartz, as indicated by the presence of SiO_2, CaO, MgO, and Al_2O_3. In terms of thermal stability, PS powder exhibits comparable properties to asbestos, with a peak degradation temperature of 745.88 °C and a total weight loss of 16 % for PS powder, versus 700 °C and 11 % weight loss for asbestos. These results suggest that PS powder could be a viable alternative to asbestos in automotive friction lining materials.

Keywords: Periwinkle shell powder, asbestos, disc brake lining, chemical, thermal and morphological properties

INTRODUCTION

There are two main types of brakes: disc brakes and band brakes. According to [1], in a typical braking system, disc brakes are usually located at the front of the vehicle, while either disc or drum brakes are used at the rear. These brakes are connected through a system of tubes and hoses that link the brakes at each wheel to the master cylinder, which is located under the

vehicle's hood. The braking system is a crucial part of an automobile and includes several components such as brake pads, the master cylinder, wheel cylinders, and a hydraulic control system [2]. The brake pads play a key role in the braking system, enabling functions such as gear shifting in automatic transmissions, as well as slowing down or completely stopping the vehicle, or keeping it stationary once stopped. When the brakes are applied, friction between the brake pads and the rotating disc causes the vehicle to stop and the vehicle's kinetic energy converted into heat. The brake pad assembly consists of steel backing plates with friction materials attached to the side facing the brake disc [3]. Brake pads (linings) are designed to provide optimal friction, stability, durability, and minimize noise and vibration.

Brake pad materials are complex, heterogeneous mixtures made up of various elements, each serving a specific purpose. These constituents work together to enhance the brake lining's performance by improving its frictional properties at both low and high temperatures, reducing noise, extending the pad's lifespan, increasing strength and rigidity, and minimizing porosity. Brake pad materials are typically classified into three main categories: organic, semi-metallic, and ceramic friction materials. These materials are generally composed of several key components, including friction additives, fillers, binders, and reinforcing fibers [4]. When combined, these components give the brake lining the necessary characteristics to function effectively.

Variations in the composition or proportions of elements used in the formulation can lead to variations in the chemical, mechanical, and physical properties of the brake pad materials [5], [6], [7] and [8]. Therefore, each new formulation must undergo a series of tests to assess its wear and friction properties. This includes on-road braking performance tests and abrasion testing to ensure that the developed brake pad lining meets the necessary standards for its intended application [9].

The development of brake friction linings has a history spanning over 100 years. The earliest brake pads were woven materials, but in the 1920s, molded materials made from chrysotile asbestos fibers an abundant mineral began to replace them. In the 1950s, resin-bonded metallic pads were introduced, and by the 1960s, semi-metallic pads with higher metal content were developed [10]. Despite these advancements, asbestos continued to be widely used in brake pad manufacturing due to its sound absorption properties, strength, flexibility, heat resistance, and resistance to electrical and chemical damage, all while remaining relatively inexpensive [11].

However, by the 1970s, concerns began to arise regarding the use of asbestos in brake pads. Studies reported that the inclusion of asbestos in commercially available brake linings was linked to cancer [12], [13] and [14]. Given its carcinogenic nature and the challenges associated with its disposal, asbestos was banned in many countries for use as a friction material [15]. This global phase-out of asbestos in automotive brake materials has driven extensive research and development into safer alternative materials to replace asbestos in brake linings.

Waste materials from industry and agriculture are gaining attention as potential alternative raw materials to asbestos in the production of brake linings [15]. Utilizing appropriate waste materials not only adds value but also helps reduce environmental issues and the costs

associated with their disposal. According to [16] the search for replacements for asbestos has led to research on various agro-wastes, including rice husk and rice straw, cashew nut shells, palm kernel shells and fibers, bagasse, coconut shells and fibers, banana peels, maize or corn husks, fly ash, cow bones and hooves, eggshells, sawdust, cocoa bean shells, seashells, and periwinkle shells, all of which are being explored as sustainable alternatives in the manufacture of eco-friendly, asbestos-free brake linings. Additionally, [17] reported the use of fan palm shells in the development of asbestos-free brake linings, while [18] highlighted the potential of bamboo fiber as a substitute for asbestos in brake lining production.

This study, therefore, explores the potential of periwinkle shell powder as a filler material in the production of brake linings, specifically investigating its suitability as a replacement for asbestos. The type of periwinkle used in this research is *Tympanotonos fuscatus* (Linnaeus, 1758), commonly known as the West African Mud Creeper, which belongs to the Potamididae family. According to [19], this species is the most common and abundant snail found in the brackish waters of West Africa. It is typically found in the lagoons and mudflats of countries such as Ghana, Nigeria, and Togo [20]. The shells of *Tympanotonos fuscatus* are elongated with progressively larger whorls, weakly curved ribs, fine striations, and blackish-brown stripes. These snails can grow to lengths of 25 mm to 95 mm and weigh between 0.02 g and 9.42 g [21]. The shells of these small gastropods are often discarded as agricultural waste, left in open fields after the flesh is removed, creating an environmental nuisance. This study examines the potential use of these shells as a viable material for automobile brake pads, while also addressing the environmental challenge posed by their accumulation.

MATERIALS AND METHODS

Source of Raw Materials

The periwinkle shell was collected from Keta, a town located along the banks of the Keta Lagoon in the Volta Region of southeastern Ghana.

Powder Preparation

The periwinkle shells used in this study were collected from a heap left in the open for over six months, allowing them to dry. Furthermore, they were sun-dried for an additional two days to reduce any remaining moisture content. Subsequently, the shells were oven-dried at 110 °C for 5 hours to ensure thorough dehydration. Initial crushing was done using a hammer. Secondary and tertiary crushing were then carried out with a Metso 4×6″ jaw crusher and a Denver 911MPE-TM-LCC21 cone crusher, respectively, to achieve particle sizes between 2 mm and 1 mm. The crushed material was subsequently milled. The charge, consisting of the pre-crushed samples, was ground for 60 minutes in a cascading BICO-type ball mill using approximately 15 kg of steel balls to produce a fine powder. After milling, the powder was screened through a 75 µm laboratory sieve (ISO3310-1:2000/BS410-1:2000 standard) to obtain the desired particle size. Figures 1 and 2 illustrate the periwinkle shell used and the resulting periwinkle powder, respectively.

Figure 1: Periwinkle shell used. Figure 2: Periwinkle shell powder.

Sample Preparation for Mechanical Tests

To prepare the samples, 150 g of periwinkle powder was mixed with 5 g of water and sodium silicate, which acted as binders. This mixture was then placed into a sample holder of a Ridsdale Standard Laboratory Sand Rammer, with dimensions of 50 mm in diameter and 50 mm in height. Three consecutive ramming blows were applied to the mixture. The compacted samples were then ejected from the holder and fired in an oven at 115 °C for 1 hour. Figure 3 displays some of the prepared samples carried out at the Sand Laboratory at the Federal Institute of Industrial Research Oshodi (FIIRO) in Lagos, Nigeria.

Figure 3: Some of the prepared samples.

Sample Analysis

The following analyses; X-Ray Fluorescence (XRF) Analysis, X-Ray Diffraction (XRD) Analysis, SEM–EDS Analysis of the Powder, DSC–TGA Analysis of the Powder, and Mechanical Characterization were conducted to establish a comprehensive understanding of the properties of Periwinkle Shell (PS) powder.

X-Ray Fluorescence (XRF) Analysis:

XRF analysis of the Periwinkle Shell (PS) powder was performed using a Genius-IF EDXRF spectrometer. Approximately 5 g of the pulverized sample was poured into a thin-film-covered sample cup, filling it to about one-third. The sample cup lids were then securely fastened to prevent any leakage or loose particles on the thin film layer. The sample was placed into the spectrometer's sample turret, and the X-ray lamp was powered on, allowing a 2-minute stabilization period. In the RUN tab, the voltage and emission current were adjusted to maintain a dead time of 35–40 kV. The analysis was then initiated at the Yaba College of Technology Laboratory in Lagos, Nigeria, to obtain the spectrum data.

X-Ray Diffraction (XRD) Analysis:
XRD analysis was conducted using a Goniometer MiniFlex 300/600 at the Materials Laboratory of the University of Lagos (UNILAG) in Nigeria. The sample material was finely ground, homogenized, and its average bulk composition determined. Analysis was carried out using a reflection-transmission spinner stage with Theta-Theta configuration. The 2θ scan started at 4° and ended at 75°, with a step size of 0.026261° and a scan duration of 8.67 seconds per step. The tube was set to a current of 40 mA and a voltage of 45 kV. A Programmable Divergent Slit with a 5 mm width mask was applied. The intensity of the diffracted X-rays was continuously recorded as both the sample and detector rotated through their respective angles.

SEM – EDS Analysis of the Powder:
At the Environmental Laboratory of UMaT, SEM imaging of the powder was performed using a Carl Zeiss EVO MA 15 Scanning Electron Microscope (SEM). A Secondary Electron (SE) detector was employed to visualize the samples under high-vacuum conditions. Energy-Dispersive X-ray Spectroscopy (EDS) was carried out using a BRUKER QUANTAX EDS system equipped with an XFlash Detector 610 M. To ensure optimal imaging due to the non-conductive nature of the samples, they were sputter-coated with a gold/palladium layer. SEM micrographs were obtained at an accelerating voltage of 4 kV, with a working distance ranging from 9.5 mm to 10 mm. The EDS spectra were recorded at an accelerating voltage of 20 kV.

DSC – TGA Analysis of the Powder:
Simultaneous DSC-TGA measurements of the powder sample were carried out using an SDT Q600 V20.9 Build 20 thermogravimetric analyzer. The sample was heated at a rate of 20 °C/min from 30 °C to a maximum temperature of 950 °C under a nitrogen flow rate of 100 mL/min. An alumina crucible was used as the reference control. The DSC/TGA curves and related data were recorded and processed using Pyris™ software on a connected computer. The tests were conducted at the Department of Materials Science and Engineering, University of Ghana.

Mechanical Characterization:
Mechanical tests conducted included untapped and dry bulk densities, as well as dry compressive and dry shear tests. The untapped bulk density test was performed using the raw powders. Approximately 100 g of the powder material was measured using a digital Ohaus analytical balance (Model PA 224) with a readability of 0.0001 g. The powder was carefully poured through a laboratory sieve with a 1.0 mm aperture into a dry 250 mL graduated cylinder, and the volume was recorded. The test was conducted in accordance with the ASTM-D7481-18 standard. Untapped bulk density was calculated by dividing the mass of the powder by the measured volume. This procedure was repeated three times at Sand Laboratory in the Foundry Department of (FIIRO), Lagos, Nigeria and the average density values were determined.

The dry bulk density test was conducted on the prepared samples (Figure 3). The weights of the samples were measured using a digital Ohaus analytical balance. The volumes were calculated based on the dimensions of the samples (50 mm diameter × 50 mm height). The dry bulk density was then determined by dividing the weight of each sample by its corresponding volume.

For the dry compression test, the prepared samples were placed between the compressive heads of a Ridsdale Universal Sand Strength Tester. A uniform load was applied until the samples fractured, and the compressive strength at the point of fracture was measured and recorded in kN/m^2. This test was conducted on three samples of the material, and the average compressive strength values were calculated and documented.

A similar procedure was followed for the dry shear test. The samples were positioned between shear heads, and a uniform load was applied until the samples sheared. The shear strength values at the point of failure were measured and recorded in kN/m^2. The average shear strength values were then calculated and documented.

RESULTS AND DISCUSSIONS

Table 1 presents the bulk densities, dry compressive strength, and dry shear strength values of the Periwinkle Shell (PS) powder. Compared to asbestos, which has a bulk density of 2.22 g/cm^3 according to [22] and a fiber density range of 2.4 – 2.6 g/cm^3 as reported by [23], the PS powder is significantly lighter. The untapped bulk density of 1.316 g/cm^3 and dry bulk density of 1.718 g/cm^3 are both lower than those of asbestos. This makes PS powder a more lightweight and potentially advantageous alternative as a filler or reinforcement material in brake linings.

Table 1: Some properties of the periwinkle shell powder.

Material	Untapped Bulk Density (g/cm^3)	Dry Bulk Density (g/cm^3)	Dry Compressive Strength (kN/m^2)	Dry Shear Strength (kN/m^2)
PS Powder	1.316	1.718	350	155

The compressive and shear strength values of the PS powder, as shown in Table 1, demonstrate its mechanical integrity and potential for structural applications. The dry compressive strength of 350 kN/m^2 indicates that the material can withstand significant compressive forces, making it suitable for use in load-bearing or impact-resistant components. Similarly, the dry shear strength of 155 kN/m^2 suggests that the material possesses adequate resistance to shear forces, which is critical for maintaining structural stability under lateral stresses.

When compared to asbestos, the PS powder offers sufficient strength for reinforcement while being significantly lighter. This combination of mechanical strength and reduced density makes PS powder an attractive alternative for manufacturing lighter yet durable components, particularly in applications such as brake pads where weight reduction is a priority without compromising performance.

Figure 4 shows the XRD pattern of the PS powder while Table 2 shows the results of the XRD quantitative analysis.

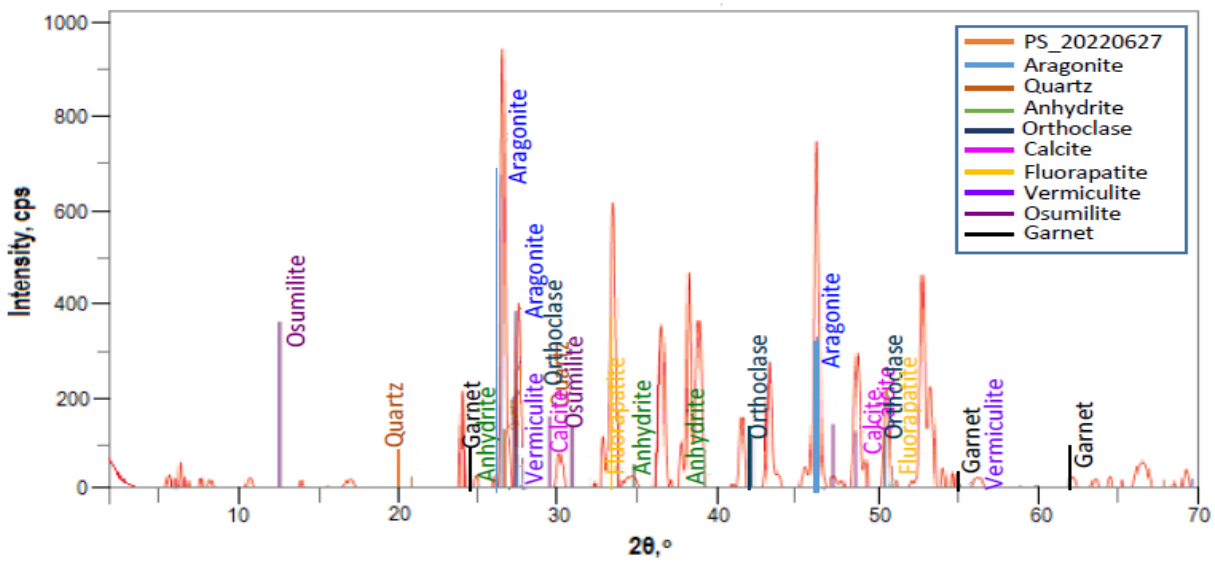

Figure 4: XRD spectrum of periwinkle shell powder.

Table 2: Quantitative analysis results of XRD of periwinkle shell powder.

DB Card Number	Space Group	Figure of Merit	Phase Name	Formular
01-085-6705	62: Pnma	0.851	Aragonite	$CaCO_3$
00-001-0649	154: P3221	1.417	Quartz	SiO_2
01-085-6126	63: Bmmb	1.668	Anhydrite	Ca (SO_4)
00-005-0518	12: C2/m	1.215	Vermiculite	Na - K - Al - O - Si.12H_2O
00-002-0475	12: C12/m1	1.376	Orthoclase	$Al_2O_3.K_2O.6SiO_2$
00-002-0629	167: R – 3c:H	1.360	Calcite	$CaCO_3$
00-002-0845	176: P63/m	1.605	Fluorapatite	(Ca F) Ca_4 (PO_4)$_3$
00-010-0413	192: P6/mcc	1.751	Osumilite	K - Na - Ca - Mg - Fe - Al - S …
00-002-0981	230: 1a – 3d	3.100	Garnet	3(Ca, Fe, Mg) O. (Al, Fe ….

Figure 4 highlights the major diffraction peaks of the PS powder, with 2θ positions observed at 26.50°, 33.42°, 38.83°, 46.16°, and 48.67°. The corresponding interplanar distances are 3.361 Å, 2.679 Å, 2.317 Å, 1.965 Å, and 1.869 Å, respectively. The primary mineral components identified at these peaks are detailed in Table 2. The XRD spectrum features clear, sharp, and narrow major diffraction peaks, indicating that the PS powder is predominantly crystalline in nature, similar to chrysotile asbestos as reported by [23].

According to [24] the mineralogy of chrysotile asbestos consists primarily of chrysotile, silica, calcite, anhydrite, and quartz. The XRD analysis of PS powder reveals the presence of the same minerals, excluding chrysotile, as shown in Table 2. These findings indicate that the PS powder and asbestos share comparable mineralogical characteristics, further suggesting the potential of PS powder as a viable alternative material.

Table 3 presents the XRF analysis results for the PS powder, alongside the XRF data for asbestos as reported by [24]. The XRF findings are consistent with the XRD results of the PS powder, confirming the alignment between both analytical techniques. Additionally, the XRF data for

the PS powder correlates with the findings of previous studies on periwinkle powder, such as those by [17] and [25], further validating the results.

Table 3: Chemical composition of PS powder from XRF.

Specification Compounds	Concentration (% weight)	
	Periwinkle Shell (PS) Powder	Asbestos
SiO_2	31.8601	34.69
Al_2O_3	11.4178	1.23
P_2O_5	0.3191	0.04
SO_3	0.3042	0.94
K_2O	0.2682	0.00
CaO	43.1553	4.16
MgO	1.7115	32.89
TiO_2	–	0.08
MnO	0.0333	0.13
Fe_2O_3	6.3855	9.46
Cr_2O_3	–	–
cl	–	–

The PS powder is found to contain silica, potassium, calcium, aluminum, and iron. These same elements are also present in the asbestos analysis data, though their concentrations vary between the two materials, as shown in Table 3. The XRF analysis confirms the presence of SiO_2, CaO, K_2O, Al_2O_3, and Fe_2O_3 as the major compounds in the periwinkle shell powder. This composition is significant for the properties of the final brake pads, as substances like SiO_2, CaO, and Fe_2O_3 are known to be among the hardest materials, according to [25]. The presence of these hard oxides, combined with the absence of radioactive elements such as Xenon (Xe), Praseodymium (Pr), and Europium (Eu) in the XRF data for the PS powder, suggests that PS powder is a suitable alternative to asbestos as a filler or reinforcement material in brake linings. The SEM micrograph and EDS spot analysis of the PS powder are shown in Figures 5.

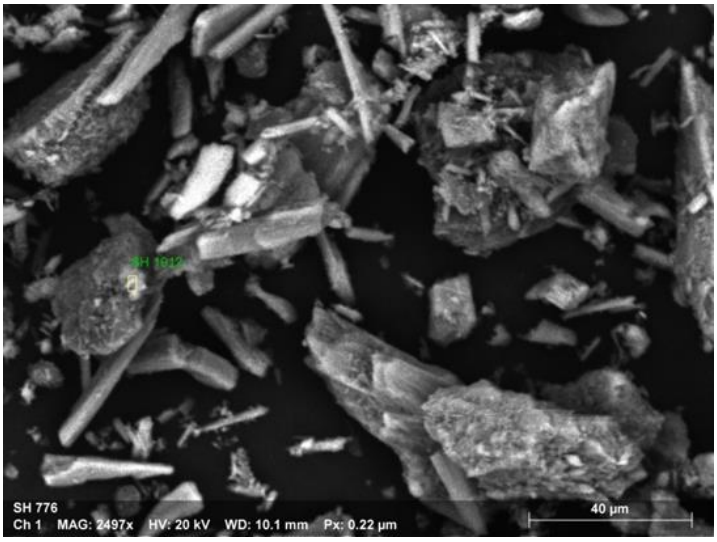

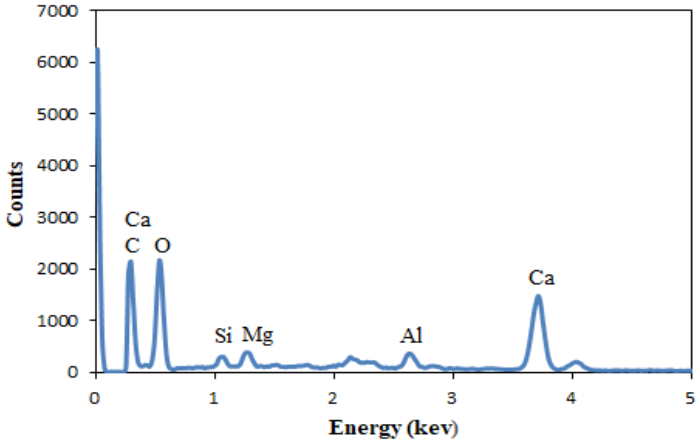

Element	At. No.	Netto	Mass [%]	Mass Norm. [%]	Atom [%]	abs. error [%] (1 sigma)	rel. error [%] (1 sigma)
Carbon	6	5327	13.22	34.54	44.07	2.07	15.67
Oxygen	8	7177	20.23	52.84	50.61	3.00	14.85
Silicon	14	442	0.31	0.81	0.54	0.05	17.67
Magnesium	12	704	0.35	0.92	0.58	0.05	14.79
Aluminium	13	696	0.24	0.63	0.27	0.04	16.02
Calcium	20	8592	3.93	10.26	3.92	0.15	3.82
		Sum	**38.28**	**100.00**	**100.00**		

Figure 5: SEM micrograph and EDS analysis of the PS powder.

The micrograph of the PS powder reveals that the particles vary in size and shape. The particles are solid and exhibit irregular sizes. A similar observation was made by [23] regarding the morphology of chrysotile asbestos. However, while asbestos fibers are thin and intertwined, they too are solid and irregular in size. The EDS elemental analysis shows that, in addition to carbon and oxygen, the PS powder contains Si, Ca, Al, and Mg. These findings align with the data obtained from the XRD and XRF analyses of the powder. Therefore, the XRD, XRF, and SEM-EDS results collectively indicate that the chemical composition of PS powder closely resembles that of asbestos.

The DSC-TGA results from the thermal analysis of the PS powder particles are presented in Figure 6.

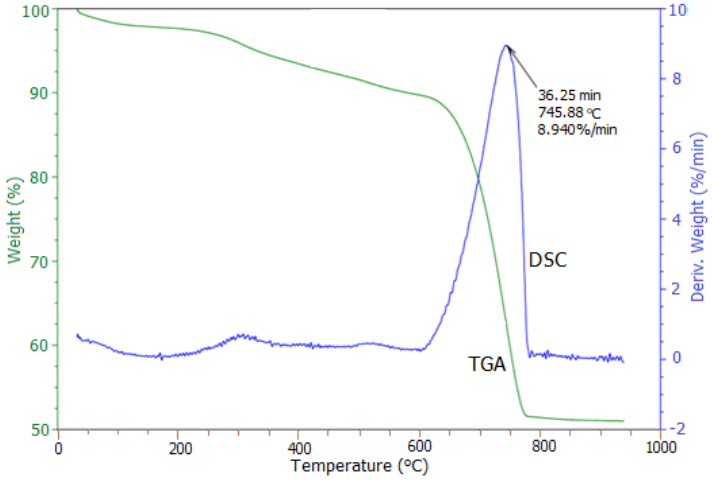

Figure 6: DSC/TGA curves of the periwinkle shell powder.

In Figure 6, the DSC analysis of the PS powder indicates that the maximum degradation occurs in a single stage, with a peak temperature of 745.88 °C and a corresponding weight loss of 36.92 %. Degradation begins at around 650 °C, accompanied by a rapid loss in mass. The TGA, in contrast, reveals three stages of weight loss: the first, from 32 °C to approximately 94 °C, is attributed to the removal of absorbed water and light volatiles; the second, from 94 °C to 400 °C, corresponds to the further removal of light volatiles; and the third, from 400 °C to about 885 °C, is due to pyrolysis.

The results of the thermal analysis of the PS powder are compared with the thermal behavior of chrysotile asbestos, as reported by [24]. Figure 7 illustrates the thermal behavior of the chrysotile asbestos sample.

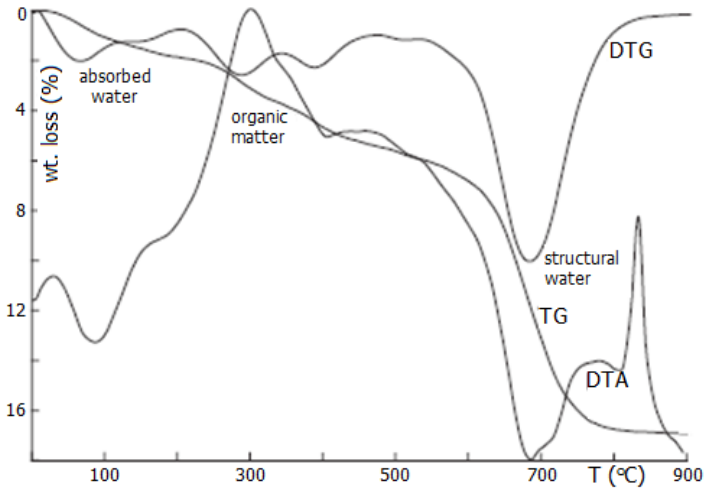

Figure 7: DTA/TG/DTG curves of chrysotile asbestos.
(Source: [24])

From Figure 7, the TG curve reveals that asbestos undergoes three distinct stages of weight loss: the first stage, up to 250 °C, corresponds to the removal of absorbed water; the second stage, between 250 °C and 500 °C, is associated with the combustion of organic matter; and the

third stage, from over 450 °C to 700 °C, involves the removal of structural hydroxyl (OH) groups from the chrysotile fibers. The maximum degradation of chrysotile occurs around 700 °C, with a weight loss of approximately 11.90 %. This finding aligns with the work of [23], who reported that chrysotile asbestos loses its chemically bonded water between 600 °C and 810 °C, leading to the complete breakdown of its mineral structure, with peak degradation temperatures ranging from 700 °C to 730 °C.

In comparison, the thermal behavior of PS powder during its first and second stages of degradation, up to 400 °C, as shown in the TGA curve, is similar to that of asbestos in its initial two stages. However, the PS powder begins to degrade at a slightly higher peak temperature (745.88 °C) compared to asbestos. Despite this, the degradation of asbestos is more gradual in its third stage, indicating that asbestos has greater heat resistance than PS powder.

The weight loss at the degradation temperatures of PS powder is comparable to that of asbestos. For instance, at 700 °C, the PS powder experiences approximately 16 % weight loss, compared to about 11.9 % for asbestos. This suggests that the PS powder offers similar thermal stability to asbestos under comparable conditions. Furthermore, according to [17], the upper operating temperature for regular street vehicles with disc brake pads typically falls within the range of 300 °C to 500 °C, which is significantly below the degradation temperatures of both PS powder and asbestos. This implies that PS powder can provide adequate thermal stability for use in brake pad applications.

The physical, chemical, morphological, and thermal analyses of the PS powder demonstrate that it shares several performance characteristics with asbestos. These findings suggest that PS powder has the potential to serve as a viable replacement for asbestos in automotive disc brake pads.

CONCLUSION

The characterization of Periwinkle Shell (PS) powder which is *noncarcinogenic* was conducted to evaluate its potential as a replacement for asbestos in brake pad linings. The morphological properties were analyzed using SEM-EDS, while thermal degradation behavior was assessed through DSC-TGA. The chemical composition and phase analysis were determined using XRF and XRD, and mechanical properties, including bulk densities, dry shear strength, and compressive strength, were also measured.

The chemical and morphological analyses revealed similarities between PS powder and chrysotile asbestos, a material commonly used in brake pad linings. Notably, the PS powder is less dense than asbestos, with bulk densities of 1.316 g/cm^3 (untapped) and 1.718 g/cm^3 (dry), compared to the 2.22 g/cm^3 bulk density of asbestos.

While asbestos begins to degrade at approximately 700 °C, the PS powder degrades at a slightly higher temperature of about 745.88 °C, indicating comparable thermal stability. Additionally, the PS powder exhibits similar degradation stages to asbestos during the initial heating phases. Based on its physical, chemical, morphological, and thermal properties, the PS powder shows strong potential as a lightweight, thermally stable, and sustainable alternative to asbestos for the production of brake linings.

References

[1]. Natarajan, M. P., et al., *Effect of ingredients on mechanical and tribological characteristics of different brake liner materials*. International Journal of Mechanical Engineering and Robotics Research, 2012. 1(2): p. 135 – 157.

[2]. Maleque, M. A., et al., *New Natural Fibre Reinforced Aluminium Composite for Automotive Brake Pad*, International Journal of Mechanical and Materials Engineering, 2012. 7(2) p. 166-170.

[3]. Aigbodion, V. S., et al., *Development of asbestos–free brake pad using bagasse.* Tribology in Industry, 2010. 32(1): p. 12.

[4]. Chan, D. and G. W. Stachowiak, *Review of automotive brake friction materials*. Proceedings of the Institution of Mechanical Engineers, D13103 © IMechE, Instn. Mech. Engrs, 2004. 218, Part D: J. Automobile Engineering.

[5]. Jang, H., et al., *Effect of Metal Fibres on the Friction Performance of Automotive Brake Friction Materials.* Wear, 2004. 256: p. 406 – 414.

[6]. Cho, M., et al., *Effect of Ingredients on Tribological Characteristics of a Brake Pad: An Experimental Case Study*. Wear, 2005. 258(11 – 12): p. 1682 – 1687.

[7]. Mutlu, I., et al., *Production of ceramic additive automotive brake lining and investigation of its braking characteristics*. Industrial Lubrication and Tribology, 2005. 57(2): p. 84 – 92.

[8]. Zaharuddin, A. M., et al., *Taguchi Method for Optimizing the Manufacturing Parameters of Friction Materials*. International Journal of Mechanical and materials Engineering, 2012. 7(1): p. 83 – 88.

[9]. Talib, R. J., et al., *The Performance of Semi-Metallic Friction Materials for Passenger Cars*. Jurnal Teknologi, 2007. 46(1): p. 53 – 72.

[10]. Nicholson, G., *Facts about Friction*: *A friction material manual, almost all you need to know about friction*. P&W Price Enterprises, Inc., 1995. Croydon, PA. p. 244.

[11]. Blau, J. P., *Compositions, Functions and Testing of Friction Brake Materials and their Additives*. A report by Oak Ridge National Laboratory, Tennessee, 37831 – 6285 for U.S. Dept. of Energy, 2001. p. 78 – 80.

[12]. Abutu, J., et al., *Production and characterization of brake pad developed from coconut shell rein forcement material using central composite design*. Springer Nature (NA) Applied Sciences, 2019. 1(82).

[13]. Dineshkumar, R., et al., *Development of friction material by using precast prefired (pcpf) blocks: Frontiers in automobile and mechanical engineering*. IOP Publishing, IOP Conf. Series: Materials Science and Engineering, 2017. 197(1): p.1 - 8.

[14]. Lawal, S. S., et al., *Development and production of brake pad from sawdust composite.* Leonardo Journal of Sciences, 2017. 30: p. 47 - 56.

[15]. Leman, Z., et al., *Moisture Absorption Behavior of Sugar Palm Fibre Reinforced Epoxy Composites*. Short Communication, International Journal of Materials and Design, 2008. 29(8): p. 95 – 100.

[16]. Abutu, J., et al., *Effects of process parameters on the properties of brake pad developed from seashell as reinforcement material using grey relational analysis*. Engineering Science Technology International Journal, 2018. 21(4): p. 787 – 797.

[17]. Amaren S. G., *Development of Automobile Disc Brake Pads using Eco-Friendly Periwinkle Shell and Fan Palm Shell Materials*. PhD Thesis, ABU, Zaria, Nigeria, 2016.

[18]. Rajaraman, K. K., et al., *Evaluation of Mechanical Properties of Brake pads prepared by organic fibres*. AIP Conference Proceedings 2311, 080004 (2020).

[19]. Reid, D. G., et al., *Mudwhelks and Mangroves: The Evolutionary History of an Ecological Association (Gastropoda Potamididae)*. Molecular Phylogenetics and Evolution, 2008. 47(2): p. 680 – 699.

[20]. Hughes, R. H., *A Directory of African Wetlands*, IUCN, ISBN 978 – 2 – 88032 – 949 – 5, 1992. P. 443.

[21]. Moruf, R. O. and A. O. Lawal-Are, *Growth Pattern, Whorl and Girth Relationship of the Periwinkle, Tympanotonus fuscatus var radula (Linnaeus, 1758) from a Tropical Estuarine Lagoon, Lagos Nigeria*. International Journal of Fisheries and Aquatic Studies, 2015. 3(1): p. 111 – 115.

[22]. Chand, N., et al., *Development of asbestos free brake pad*. IE (I) Journal - MC, 2004. 85: p. 13 – 16.

[23]. Kusiorowski, R., et al., *Thermal decomposition of different types of asbestos*. Journal of Thermal Analysis and Calorimetry, 2012. 109: p. 693 – 704.

[24]. Dellisanti, F., et al., *Experimental results from thermal treatment of asbestos containing materials*. GeoActa, 2002. 1(61): p. 61 – 70.

[25]. Aku, S. Y., et al., *Characterization of periwinkle shell as asbestos free brake pad material*. Pacific Journal of Science and Technology, 2012. 13(2): p. 57 - 62.